Bull. Mater. Sci., Vol. 29, No. 5, October 2006, pp. 505–511. © Indian Academy of Sciences.

Optimizing growth conditions for electroless deposition of Au films on Si(111) substrates

BHUVANA and G U KULKARNI*
Chemistry and Physics of Materials Unit and DST Unit on Nanoscience, Jawaharlal Nehru Centre for Advanced Scientific Research, Jakkur PO, Bangalore 560 064, India

MS received 24 March 2006

Abstract. Electroless deposition of Au films on Si(111) substrates from fluorinated-aurate plating solutions has been carried out at varying concentrations, deposition durations as well as bath temperatures, and the resulting films were characterized by X-ray diffraction, optical profilometry, atomic force microscopy and scanning electron microscopy. Depositions carried out with dilute plating solutions (< 0·1 mM) at 28°C for 30 min produce epitaxial films exhibiting a prominent Au(111) peak in the diffraction patterns, while higher concentrations or temperatures, or longer durations yield polycrystalline films. In both epitaxial and polycrystalline growth regimes, the film thickness increases linearly with time, however, in the latter case, at a rate an order of magnitude higher. Interestingly, the surface roughness measured using atomic force microscopy shows a similar trend. On subjecting to annealing at 250°C, the roughness of the film decreases gradually. Addition of poly (vinylpyrrolidone) to the plating solution is shown to produce a X-ray amorphous film with nanoparticulates capped with the polymer as evidenced by the core-level photoelectron spectrum. Nanoindentation using AFM has shown the hardness of the films to be much higher (~ 2·19 GPa) than the bulk value.

Keywords. Electroless deposition; nanoindentation; surface morphology.

1. Introduction

Electroless deposition of metals on semiconductor surfaces is an important topic in view of its application in electronics (Khoperia *et al* 1997; Okinaka *et al* 1998; Osaka *et al* 2003), surface coatings (Pearlstein and Lawenheim 1974; Mallory and Hajdu 1990) and nanofabrication (Sugimura and Nakagiri 1995; Kobayashi *et al* 2000). By definition, it requires no external potential and the deposition is carried out usually in a fluoride solution, by the reduction of metal ions at a semiconductor surface. The half-cell reactions on a Si substrate are as follows:

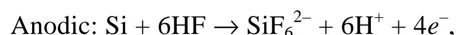

Anodic: $Si + 6HF \rightarrow SiF_6^{2-} + 6H^+ + 4e^-$,

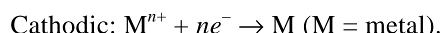

Cathodic: $M^{n+} + ne^- \rightarrow M$ (M = metal).

The advantages of electroless deposition are many: it is simple, relatively inexpensive and does not generally depend on the shape, size or conductivity of the substrate but yields high purity films. Using electroless deposition, several metals have been deposited on Si and Ge surfaces that include Cu (Nagahara *et al* 1993; Morinaga *et al* 1994; Norga *et al* 1997; Homma *et al* 1998; Magagnin *et al* 2001, 2003), Ni (Furukawa and Mehregany 1996; Gorostiza *et al* 2000; Li *et al* 2005), Al (Nagahara *et al* 1993), Sn (Nagahara *et al* 1993), Pd (Nagahara *et al* 1993), Pt (Gorostiza *et al* 1996, 1997; Kuznetsov *et al* 2001), Ag (Shacham-Diamond *et al* 2000; Kalkan and Fonash 2005) and Au (Krikshtopaitis and Kudzhmauskaite 1971; Nagahara *et al* 1993; Magagnin *et al* 2002; Warren *et al* 2002). Magagnin *et al* (2001) reported improved adhesion of Cu films on Si substrates when sodium sulfate or ascorbic acid is added to the plating solution. They also examined the films by microindentation (Magagnin *et al* 2003). Homma *et al* (1998) monitored using STM, the nucleation and growth of Cu on Si(111). Mechanism of Cu ion reduction on Si in dilute HF solution has been discussed by Norga *et al* (1997). Gorostiza *et al* (2000) studied the electroless deposition of Ni on Si substrates by varying pH of the plating solution. At pH of 1·2, no deposition was seen while at pH of 8·0, the Ni deposition was found to be rich. Furukawa and Mehregany (1996) have shown that optimal conditions of temperature and pH are necessary to obtain smooth Ni films. The effect of HF concentration on the initial stages of the electroless deposition of Al, Au, Cu, Sn and Pd on Si(100), has been carefully studied by Nagahara *et al* (1993) using atomic force microscopy. The rate of metal deposition on the nature of the dopant has also been studied. For equal deposition times, more Pt was found to be deposited on *p*-Si substrates than on *n*-Si substrates (Gorostiza *et al* 1997). In some cases such as Pt on *p*-Si(100), both metal and its silicide have been detected (Gorostiza *et al* 1996). Recently, Kalkan and Fonash

*Author for correspondence (kulkarni@jncasr.ac.in)

(2005) reported Ag nanoparticle ensembles on nanostructured Si films. Deposition of Au films from fluoride solutions on Si and Ge surfaces has been studied by Krikshtopaitis and Kudzhmauskaite (1971) about thirty years ago. Magagnin *et al* (2002) examined the orientation and chemical nature of the metal at Au–Si and Au–Ge interfaces. Using atomic force microscopy and surface diffraction, Warren *et al* (2002) studied the Au cluster formation as a function of concentration of the plating solution. The deposited films of Au, especially of (111) orientation have been evaluated as substrates for organizing self-assembling molecules (Hou *et al* 1998, 1999).

We considered it interesting to investigate Au films on Si(111) surface prepared by electroless deposition under different plating conditions. For this purpose, we used plating solutions containing different concentrations of the gold precursor ($KAuCl_4$) and varied the rate of deposition as a function of time and temperature. An important finding from this part of the study is the set of optimal conditions to obtain well-oriented Au(111) films. We have monitored the orientation of the films using X-ray diffraction (XRD) and the surface morphology by atomic force microscopy (AFM). Nanoindentation using AFM was performed to determine the hardness. We have studied the growth process by measuring the film thickness using an optical profiler (OP). Furthermore, we have examined the effect of annealing at elevated temperatures for different durations. The influence of an additive to the plating solution, poly(vinylpyrrolidone), has also been examined. The composition of films in such cases was obtained using X-ray photoelectron spectroscopy (XPS). Thus, our study forms a systematic approach to Au plating on Si substrates.

2. Experimental

The Si(111) substrates were cleaned by sonicating in acetone and double distilled water and were UV irradiated at room temperature for 15 min. They were cleaned further by heating at 80°C in piranha solution (1 : 2 H_2O_2 : H_2SO_4) (Caution: this mixture reacts violently with organic matter) for 10 min. Prior to deposition, the substrate was etched in concentrated HF for 10 min, rinsed with double distilled water and dried under flowing argon. Immediately after, it was dipped without stirring in a fresh plating solution (5 mL) of $KAuCl_4$ in 5M HF with the concentration varying in the range 0·02–5 mM, taken in a teflon container. After a certain interval of time (30–150 min), the substrate deposited with the Au film was carefully rinsed with double distilled water and dried under argon. The film deposition has been carried out at various bath temperatures (0–60°C). In some cases, the as-prepared samples were subjected to annealing up to 300°C. Further in this study, the plating solution was added with surfactant, poly(vinylpyrrolidone) (PVP, M_W ~ 40,000 g mol^{-1}) in the concentration range 0·005–0·1 mM. The conditions employed for preparing the different samples are listed in table 1.

XRD measurements were performed on a Miniflex (Rigaku, Japan) (Cu K_α, 1·5406 Å; scan rate, 1 deg/min). AFM measurements were made using a Digital Instruments Multimode head attached to a Nanoscope-IV controller (Veeco, USA). Standard Si_3N_4 cantilevers were used for the normal topography and friction mode imaging in contact mode, and for the tapping mode, etched silicon cantilevers were employed. The rms roughness values were obtained from the image analysis tools available with the instrument.

Table 1. The plating conditions for various films.

Sample number	$KAuCl_4$ (mM)	Time of deposition (min)	Bath temperature (°C)	PVP additive (mM)
1	0·02			
2	0·2	↓		
3	0·5	30		
4	1·0	↑		
5	5·0			
6		5	↓	
7		10	28	
8		15	↑	
9		20		
10		45		
11		60		
12	↓	90		
13	0·1	120		
14	↑	150		
15			0	
16		↓	60	
17		30	↓	0·005
18		↑	28	0·01
19			↑	0·04
20				0·1

Nanoindentation experiments were performed in the tapping mode using a cantilever carrying a pyramidal diamond tip (spring constant, 278 Nm^{-1} and resonance frequency, 52·8 Hz). The indentation impression was also imaged with the same tip. The hardness was calculated from the load-displacement data obtained by nanoindentation. The Au(4f) core-level spectra were collected using ESCALAB MK-IV spectrometer with an Al K_a source (1486·6 eV). For thickness measurement, a step was created by partially dipping the Si substrate vertically in the plating solution. Thickness measurements were performed using a Wyko NT1100 optical profiler (Veeco, USA).

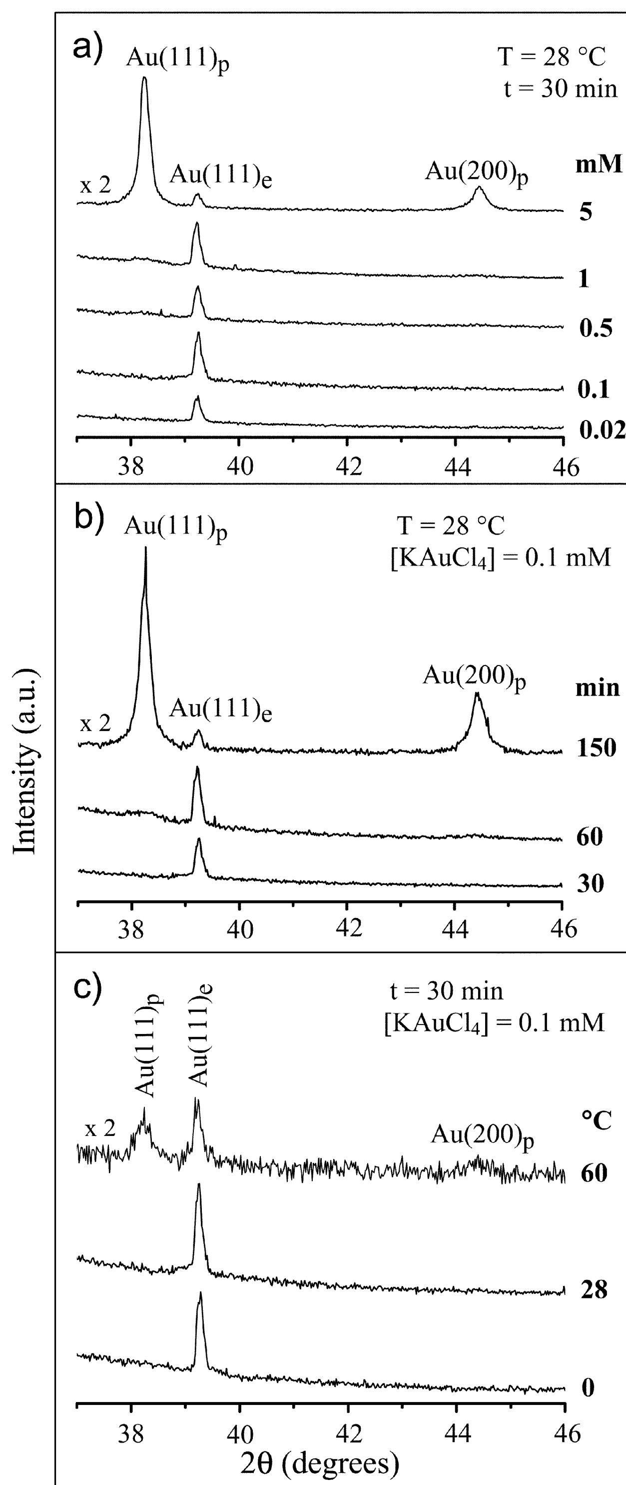

Figure 1. X-ray diffraction patterns of Au films deposited on Si(111) substrates while varying (**a**) concentration of $KAuCl_4$, (**b**) deposition time and (**c**) bath temperature.

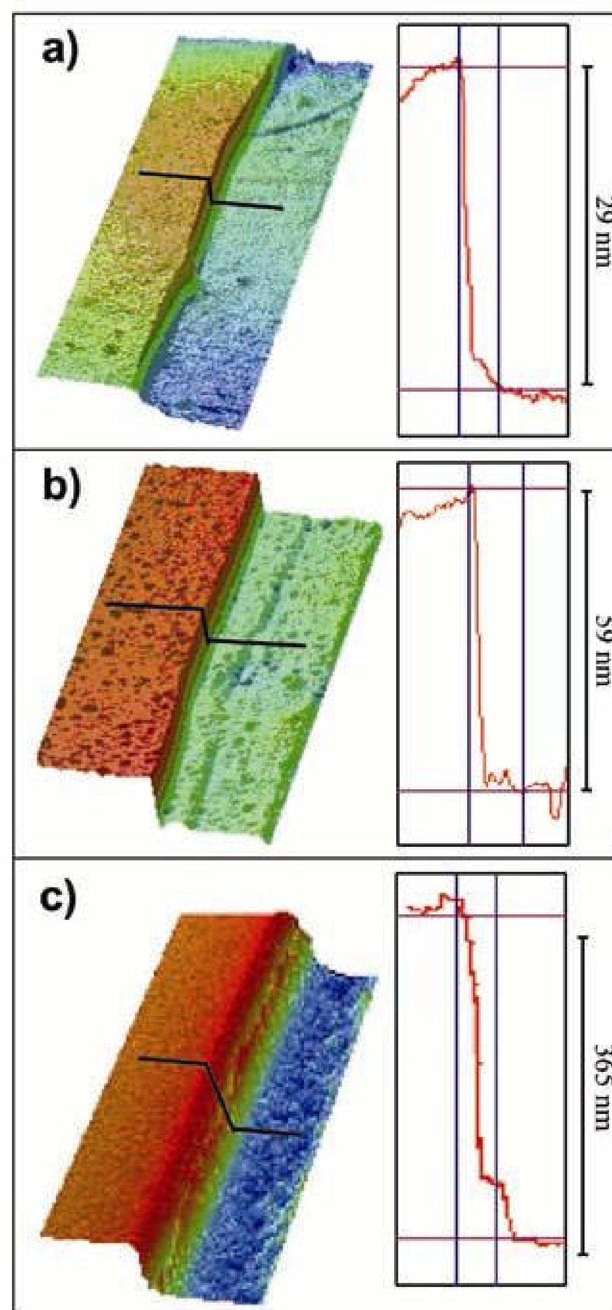

Figure 2. Profilometric measurements on Au films obtained by dipping Si substrates in the plating solution for (**a**) 30 min, (**b**) 60 min and (**c**) 90 min. The deposition was carried out under standard plating conditions (0·1 mM $KAuCl_4$, 28°C).

3. Results and discussion

X-ray diffraction patterns of the Au films obtained under different deposition conditions are shown in figure 1. As shown in figure 1a, for small concentrations of the aurate ion, say 0·02 mM, with a deposition time of 30 min at 28°C (sample 1, see table 1), we see only one peak in the diffraction pattern at 2θ of 39·2° corresponding to *d*-spacing of 2·295 Å, matching closely with the d_{111}-spacing of the bulk Au (2·355 Å). Similar observation has been made by Kuwahara *et al* (1994), who reported a difference in the *d*-spacing of 0·04 Å for the epitaxial Au film on Si(111) grown by vacuum deposition. The intensity of the (111) diffraction peak grows gradually as the concentration of aurate ion is increased from 0·02 to 1 mM (samples 1–4) with no evidence of other diffraction peaks. At higher concentrations (5 mM, sample 5), however, we observe additional peaks at 38·24° and 44·42° corresponding to bulk Au spacings of d_{111} (2·350 Å) and d_{200} (2·039 Å), respectively. The peak at 2·295 Å from the lower epitaxial layer is much reduced in intensity. In figures 1b and c are shown the diffraction patterns obtained while varying the time of deposition and the bath temperature, respectively. Clearly, longer deposition durations and higher temperatures yield polycrystalline Au films. It may be noted from the intensity of (111) peak in the diffraction patterns that the amount of deposition is considerably low for deposition carried out at 60°C (sample 16), while for 0°C (sample 15) the intensity is comparable to the room temperature deposition (sample 2) (see figure 1c). Our study shows that among the various parameters, the deposition time gives a good control on the thickness of film.

As shown in figure 2, the Au films obtained from a bath containing 0·1 mM $KAuCl_4$ at 28°C, for 30, 60 and 90 min (samples 2, 11 and 12) exhibit steps of 29, 59 and 365 nm, respectively with respect to the Si substrate. Using AFM, we found the rms roughness of the films to be 7·9, 12·8 and 17·1 nm, respectively. Naturally, this sets a lower limit of thickness for a uniform Au film. In other words, the thickness of the film deposited by this method could be controlled within a few nanometres by varying the deposition time. Figure 3 shows that the rate of deposition as measured by OP, varies proportionally with time. During the first hour, the deposition is at the rate of 1·03 nm/min (samples 2, 6–11) and at longer durations, there is almost an order of magnitude rise, 9·04 nm/min (samples 12–14). Referring to figure 1b, it is interesting to note that this change of behaviour in the film coincides with epitaxial growth of the film becoming polycrystalline. The rms roughness values obtained from contact AFM (see figure 3) also exhibit a similar trend, implying that a change in the rate of deposition owes much to the increased roughness from polycrystallinity.

In order to improve the texture, the film (sample 2) was subjected to annealing at elevated temperatures of 250°C and 300°C. In figure 4 are shown AFM and diffraction measurements after annealing at 250°C for different time durations. As seen from figure 4a, the deposited film is granular and the particulates appear agglomerated into islands measuring hundreds of nanometres. Annealing at 250°C for 2 h (figure 4b) improved the surface topography. With further annealing for 10 h, the particles measuring ~ 35 nm appear closely packed. Additional annealing, however, makes the particles grow almost three times bigger (see figure 4d). The roughness values obtained from AFM analysis (see inset of figure 4) show a sharp decrease from ~ 12 to ~ 5 nm following annealing. Interestingly, the (111) oriented nature of the film remains almost unaffected as evident from the X-ray diffraction patterns shown along with the images. However, the film became essentially polycrystalline after annealing at 300°C for 1 h.

We have made a detailed study on the influence of surfactant on the gold deposition. For this purpose, PVP was added in small concentrations under the standard plating conditions (0·1 mM $KAuCl_4$, 28°C, 30 min) and the results obtained are shown in figure 5. At smaller concentrations of PVP, 0·005 and 0·01 mM (samples 17 and 18, respectively), the diffraction patterns in figure 4a resemble closely with those without the additive (see figure 1a). In other words, the presence of PVP brings no noticeable change in the diffraction patterns at such low concentrations. In contrast, for higher concentrations, ≥ 0·04 mM (samples 19 and 20), there is hardly any intensity in the diffraction pattern, as if the deposition process itself is hindered. The nature of the deposited material became more evident from the AFM and XPS analysis shown in figures 5b and c. The AFM image in figure 5b reveals the granular structure of the deposited material, with granules in the range of 80–140 nm. Each granule appears as an aggregate of particulates

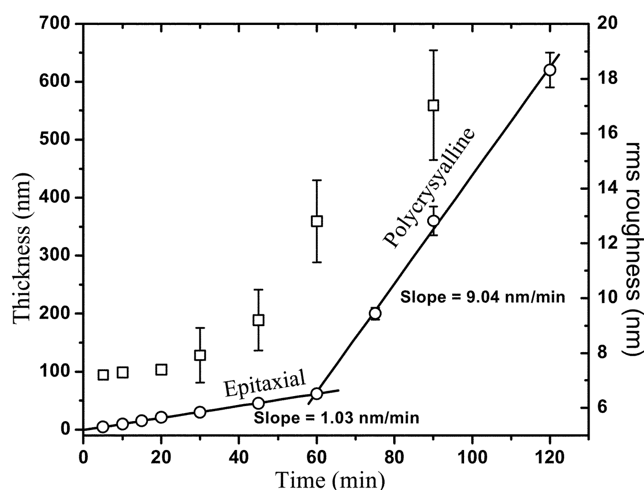

Figure 3. Variation in the thickness of the films (circles) as a function of time in the standard plating solution (0·1 mM $KAuCl_4$, 28°C). The variation in the rms roughness values (squares) estimated from $2 \times 2\ \mu m^2$ area using AFM, is also shown.

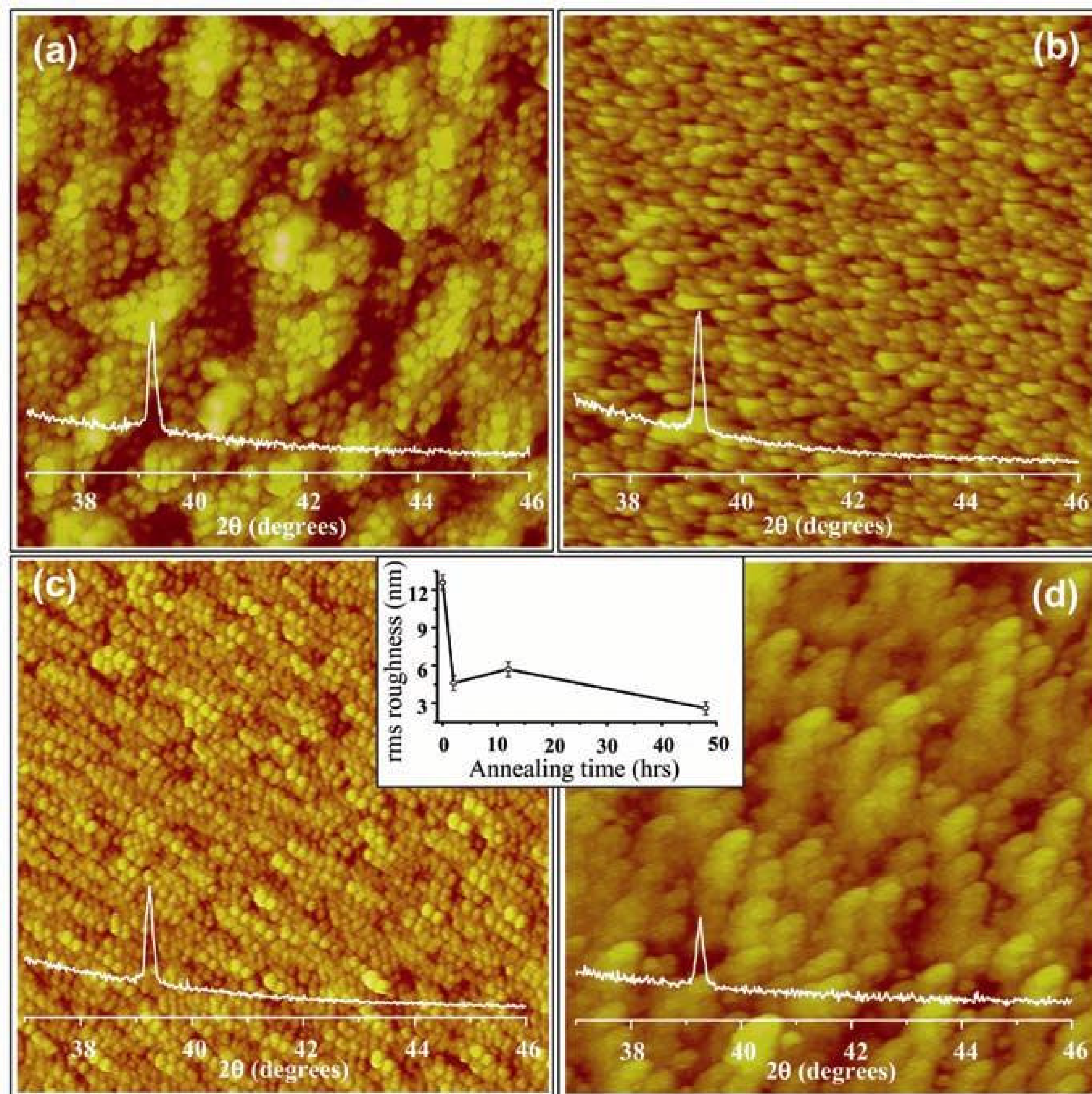

Figure 4. Tapping mode AFM images ($2 \times 2\ \mu m^2$) obtained after annealing an Au film at 250°C for different time durations: (**a**) as prepared (0 h), (**b**) 2 h, (**c**) 12 h and (**d**) 48 h. Variation in the rms roughness values estimated from AFM analysis is shown in the centre. The film was prepared under standard plating conditions (0·1 mM $KAuCl_4$, 28°C, 30 min). In each case, the corresponding XRD patterns are shown.

each presumably only a few nanometers in size (see inset in figure 5b). The Au($4f$) core level obtained from the films indeed revealed the presence of Au^0 and Au^{1+} species as illustrated in figure 5c for a PVP concentration of 0·1 mM (sample 20). Clearly, the Au^{1+} species arises due to capping of PVP due to surface Au–N or Au–C bonds (Tsunoyama *et al* 2004). The Au^{1+} concentration in the film increases with the concentration of PVP in the plating solution as shown in the inset of figure 5c. It is possible that PVP arrests the growth of Au particulates, more so when it is in higher concentrations, rendering the film X-ray amorphous.

The mechanical properties of Au films have been measured by nanoindentation (Salmeron *et al* 1992; Tan-

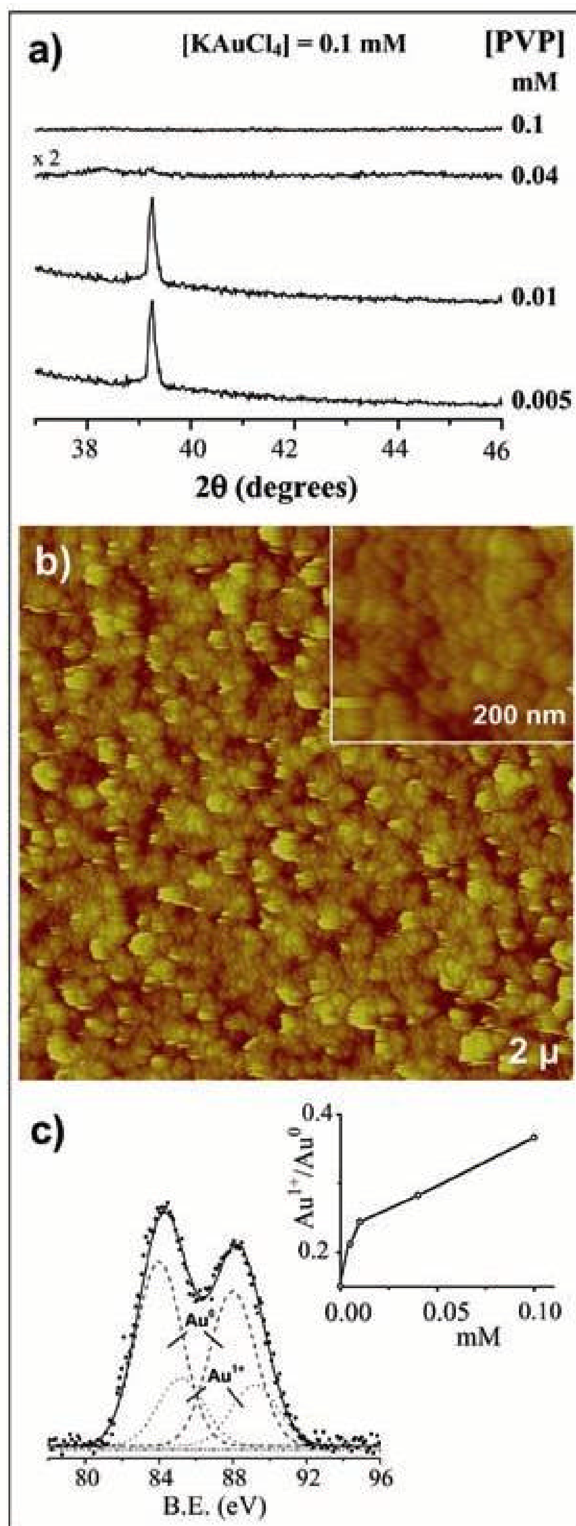

Figure 5. (**a**) XRD patterns of Au films obtained with different concentrations of poly (vinylpyrrolidone) (PVP) under the standard plating conditions (0·1 mM $KAuCl_4$, 28°C, 30 min), (**b**) tapping mode AFM image of an Au film for a PVP concentration of 0·1 mM. Inset shows an image from a smaller scan area and (**c**) Au(4*f*) core-level spectrum of the film. The presence of Au^{1+} and Au^0 species is revealed following Gaussian fitting. Inset shows variation in Au^{1+}/Au^0 with PVP concentration.

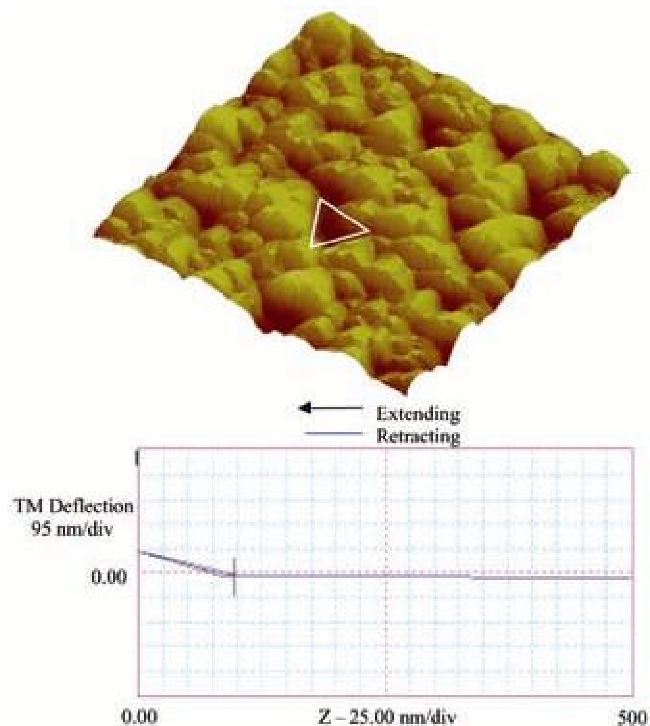

Figure 6. Tapping mode image of the film (sample 2) ($1 \times 1\ \mu m^2$) showing the indented region. The corresponding *F*–*d* curve is shown below.

gyunyong *et al* 1993; Volinsky *et al* 2004; Šiller *et al* 2005). Figure 6 shows the AFM image of an indented region (sample 2, see table 1) along with the force-distance response. The projected area of the indented surface is estimated to be 8321 nm^2. The hardness was calculated using the formula,

$$H = F/A,$$

where *F* is the applied force and *A*, the projected area of indentation (Arnault *et al* 2002). The estimated hardness of the Au film is $2{\cdot}19 \pm 0{\cdot}1$ GPa. While bulk Au has much lower hardness (0·64 GPa), the obtained value may be compared with the hardness of sputtered Au films (2·01 GPa) (Šiller *et al* 2005).

4. Conclusions

The present study has for the first time, established experimental conditions optimal for electroless deposition of Au(111) films of desired thickness. Thus, deposition carried out with a plating solution ($KAuCl_4$ in 5M HF) with 0·1 mM of $[AuCl_4]^-$ ions at room temperature for 30 min, produces a well-oriented film of thickness, ~ 29 nm. Higher precursor concentrations, higher temperatures and longer deposition times produce polycrystalline films with increased roughness. For a given concentration of the precursor (0·1 mM), the film thickness is found to increase linearly

with time (~ 1 nm/min) during the first hour and the growth became much faster at longer durations (~ 9 nm/min), with the film texture turning polycrystalline. Annealing a well-oriented film at 250°C for 12 h reduces the roughness. We have found that PVP as additive to the plating solution, greatly influence the morphology of the resulting films. It produces X-ray amorphous films containing Au^{1+} species proportional to the PVP concentration itself as evidenced by X-ray photoelectron spectroscopy. The estimated hardness ($2{\cdot}19 \pm 0{\cdot}1$ GPa) from nanoindentation is similar to that of the sputtered films.

Acknowledgements

The authors are grateful to Prof. C N R Rao, for useful discussions and encouragement. They thank Dr Gargi Raina, S J Neena and T Vijaykumar for their assistance in measurements. Thanks are also due to Veeco India Nanotechnology Laboratory, JNCASR, for providing the Optical Profiler Facility.

References

Arnault J C, Mosser A, Zamfirescu M and Pelletier H 2002 *J. Mater. Res.* **17** 1258

Furukawa S and Mehregany M 1996 *Sensors & Actuators* **A56** 261

Gorostiza P, Servat J, Morante J R and Sanz F 1996 *Thin Solid Films* **275** 12

Gorostiza P, Diaz R, Servat J, Sanz F and Morante J R 1997 *J. Electrochem. Soc.* **144** 909

Gorostiza P, Kulandainathan M, Diaz R, Sanz F, Allongue P and Morantes J R 2000 *J. Electrochem. Soc.* **147** 1026

Homma T, Wade C P and Chidsey C E D 1998 *J. Phys. Chem.* **B102** 7919

Hou Z, Abbott N L and Stroeve P 1998 *Langmuir* **14** 3287

Hou Z, Dante S, Abbott N L and Stroeve P 1999 *Langmuir* **15** 3011

Kalkan A K and Fonash S J 2005 *J. Phys. Chem.* **B109** 20779

Khoperia T N, Tabatadze T J and Zedgenidze T L 1997 *Electrochimica Acta* **42** 3049

Kobayashi T, Ishibashi J, Mononobe S, Ohtsu M and Honma H 2000 *J. Electrochem. Soc.* **147** 1046

Krikshtopaitis I B and Kudzhmauskaite Z P 1971 *Elektrokhimiya* **7** 1679

Kuwahara Y, Natatani S, Takahasi M, Aono M and Takahashi T 1994 *Surf. Sci.* **310** 226

Kuznetsov G V, Skryshevsky V A, Vdovenkova T A, Tsyganova A I, Gorostiza P and Sanz F 2001 *J. Electrochem. Soc.* **148** C528

Li L B, An M Z and Wu G H 2005 *Mater. Chem. Phys.* **94** 159

Magagnin L, Maboudin R and Carraro C 2001 *Electrochem. Solid State Lett.* **4** C5

Magagnin L, Maboudian R and Carraro C 2002 *J. Phys. Chem.* **B106** 401

Magagnin L, Maboudian R and Carraro C 2003 *Thin Solid Films* **434** 100

Mallory G O and Hajdu J B (eds) 1990 *Electroless plating: Fundamentals and applications* (Orlando, Florida: AESFS)

Morinaga H, Suyama M and Ohmi T 1994 *J. Electrochem. Soc.* **141** 2834

Nagahara L A, Ohmori T, Hashimoto K and Fujishima A 1993 *J. Vac. Sci. Technol.* **A11** 763

Norga G J, Platero M, Black K A, Reddy A J, Michel J and Kimerling L C 1997 *J. Electrochem. Soc.* **144** 2801

Okinaka Y and Hoshino M 1998 *Gold Bull.* **31** 3

Osaka T, Takano N and Yokoshima T 2003 *Surf. Coating Tech.* **169–170** 1

Pearlstein F and Lowenheim F A (ed.) 1974 *Modern electroplating* (New York: Wiley)

Salmeron M, Folch A, Neubauer G, Tomitori M, Ogletree D F and Kolbe W 1992 *Langmuir* **8** 2832

Shacham-Diamond Y, Inberg A, Sverdlov Y and Croitoru N 2000 *J. Electrochem. Soc.* **147** 3345

Šiller L, Peltekis N, Krishnamurthy S and Chao Y 2005 *Appl. Phys. Lett.* **86** 221912

Sugimura H and Nakagiri N 1995 *J. Vac. Sci. Technol.* **B13** 1933

Tangyunyong P, Thomas R C, Houston J E, Michalske T A, Crooks R M and Howard A J 1993 *Phys. Rev. Lett.* **71** 3319

Tsunoyama H, Sakurai H, Ichikuni N, Negishi Y and Tsukuda T 2004 *Langmuir* **20** 11293

Volinsky A A, Moody N R and Gerberich W W 2004 *J. Mater. Res.* **19** 2650

Warren S *et al* 2002 *Surf. Sci.* **496** 287